

## **A 3D seismic travelttime tomography study of the shallow subsurface at the CO<sub>2</sub>SINK project site, Ketzin, Germany**

Sawasdee Yordkayhun, Ari Tryggvason and Christopher Juhlin

Department of Earth Sciences, Uppsala University, Villavägen 16, SE-75236 Uppsala, Sweden

### **Abstract**

3D seismic travelttime tomography is tested at the CO<sub>2</sub>SINK project site, a small scale storage and monitoring project of CO<sub>2</sub> injection into a saline aquifer formation near the town of Ketzin, Germany. The main purpose of this study is to obtain additional information on the inhomogeneous near-surface layers above 150 ms where the 3D reflection seismic image is poor.

First arrival traveltimes from a subset of the 3D reflection data were used for this study. We use a 3D travelttime tomography technique based on a combination of solving for 3D velocity structure and static corrections in the inversion process. The resulting velocity model shows low velocities of 800-1000 m/s in the cover of the study area. A velocity contrast of approximately 1600 m/s and 2000 m/s at 60-80 m depth represents the boundary between Quaternary deposits and Tertiary sections. Correlation of the tomographic images with a similarity attribute slice at 150 ms (about 150 m depth) indicates that east-west running fault zones observed in the reflection data may extend into the Tertiary sections. This is shallower than what can be mapped from the reflection seismic images.

## 1. Introduction

Significant increasing levels of greenhouse gases in the atmosphere, especially CO<sub>2</sub>, is believed to be the main factor contributing to global warming. A rapid response to reducing greenhouse gas emissions is the technology of CO<sub>2</sub> capture and storage, in particular geological storage (Arts et al., 2004). Aside from capture and storage, the monitoring of long term CO<sub>2</sub> migration after injection is of critical importance for safety and public confidence in the technology. The CO<sub>2</sub>SINK project is an European Union research and development project which was initiated in 2004 (Förster et al., 2006). It consists of small scale storage and monitoring of CO<sub>2</sub> that is injected into a saline formation near the town of Ketzin, Germany. In autumn 2005, a 3D baseline seismic survey covering about 12 km<sup>2</sup> of the subsurface was acquired as part of the project (Juhlin et al., 2006). The survey aimed to provide (1) an understanding of the structural geometry for flow pathways within the reservoir, (2) a baseline for later evaluation of the time evolution of rock properties as CO<sub>2</sub> is injected into the reservoir, and (3) detailed subsurface images near the injection borehole for planning of the drilling operations.

In the 3D seismic survey, the processing scheme has focused on obtaining detailed information on the target, in particular, the locations of the planned injection and observation boreholes that will be drilled into the saline sandstone aquifer of the Upper Triassic Stuttgart Formation (about 600 m depth in an anticlinal structure). The preliminary results clearly show a series of distinct reflections, including a dominant reflection from within the caprock horizon (K2) lying over the Stuttgart Formation. Clear reflections are seen in the seismic volume as shallow as up to the base of the Tertiary at about 150 ms. Possible fault zones are also observed in the northern part of the area. Although these zones are situated rather far away from the planned injection borehole, they are of interest in that shallower levels of the anticline (about 250-400 m depth) have been used for storage of natural gas up to year 2000. Gas induced amplitude brightening has been observed along some of these fault zones, indicating that the stored natural gas has migrated along the fault zones at some stage. The reflection seismic images shallower than about 150 ms have poor resolution due to the acquisition geometry, frequency limitations of the data and some artefacts of the data processing. Thus, the boundary between the Quaternary and Tertiary sections, the extension of the fault zones and possible gas migration along the fault zones have not been imaged in the reflection processing. Therefore, we have focused our tomography study on this area of the survey in order to fill the gap between the deeper and shallower parts of the subsurface.

Previous work on the shallow subsurface at this site included first arrival traveltimes inversion of a 2D seismic pilot survey conducted in 2004 (Yordkayhun et al., 2006). The resulting velocity-depth models show a vertical velocity variation corresponding to the sedimentary sequences present in this area. This study also showed that the thickness variations of the low velocity unconsolidated sediment in the topmost layer yielded variations in the travel times (statics) larger than the estimated picking errors. Controllable in 2D, a more sophisticated technique is needed for the 3D data in order to prevent the near surface variation from manifesting as artefacts in the deeper layers.

In recent years, seismic tomography has become a standard tool to determine the velocity variation in complex geological environments. Originally developed for earthquake data, controlled source tomographic applications range from identifying near-surface fracture zones in hard rock environments (e.g., Bergman et al., 2004; 2006), paleochannel mapping (e.g., Deen and Gohl, 2002), and contamination site investigations (e.g., Zelt et al., 2006). In addition to conventional tomography (velocity imaging), we solve for a static term simultaneously in order to handle the near-surface weathering layer.

## 2. Data

First arrival traveltimes were picked from 344 shots in two templates of the 3D reflection data with a maximum recorded offset of about 1000 m. A weight drop was used as a source and the receivers were placed at about 20-30 cm depth. Automatic picking was performed in linear moveout panels with a wide bandpass filter applied to remove the low and high

frequency noise. Due to the presence of ground roll on the near offset traces and ambient noise in the far offset traces, these parts of data picking were refined manually.

*A priori* information from boreholes and the velocity model from the 2D pilot study in this area provided a 1D starting model for the 3D traveltimes tomography. Two starting models were tested with the same inversion parameters in order to check the robustness of the method in response to the distribution of the raypaths in the velocity models. The two models similarly consist of a low velocity cover (900-1000 m/s) that is 20 m thick. Below this depth the velocities rapidly change from 1000 to 1600 m/s and from there the velocity increases either gradually (about 50 m/s/m) or in a discontinuity at 100 m depth to 1700-2000 m/s (Figure 1a).

### 3. Method

The short-wavelength variations in the first arrivals caused by near surface variations must be handled in order to reduce the number of artefacts in the velocity model. Bergman et al., (2004; 2006) have demonstrated and successfully applied a tomography technique based on a combination of solving for velocity structure and static corrections in the inversion process. The method was fully 3D, though the dataset they used had a 2D crooked line geometry and was acquired in a hard rock environment. We now test the method for the first time for a real 3D data set acquired in a sedimentary environment.

The forward calculation of traveltimes in the model is computed using a first-order finite-difference approximation of the eikonal equation (Podvin and Lecomte, 1991; Tryggvason and Bergman, 2006). Once the traveltimes to all receivers (or shots) are computed, the raypaths are computed by ray tracing backward from receiver locations perpendicular to the isochrones (Hole, 1992). The model parameterization is performed by dividing the model into uniform block sizes of  $20 \times 20 \times 5$  m in the x, y and z direction, respectively. The equation of the traveltime residual ( $r_{ij}$ ) for all  $I$  shots and  $J$  receivers after linearizing and parameterizing the traveltime equation about starting model is given by

$$r_{ij} = s_i + \sum_n \frac{\partial T_{ij}}{\partial u_n} \Delta u_n, \quad i = 1, \dots, I, \quad j = 1, \dots, J \quad (1)$$

where  $s_i$  is the shot static correction to the traveltime,  $\partial T_{ij}/\partial u_n$  is the partial derivative of traveltime  $T_{ij}$  with respect to the slowness in block  $n$  along the raypath, and  $\Delta u_n$  is the change in slowness in model block  $n$  that is to be found for all  $N$  blocks. Eq. 1 is solved in the least-squares sense iteratively by the conjugate gradient solver LSQR (Paige and Saunders, 1982). Obviously Eq. 1 is not complete, as there should also be a receiver static term. The method can, however, not produce both at the same time, thus in between iterations the derived source statics are distributed between all the sources and receivers according to a similar scheme described by Bergman et al. (2006). In this study, all inversions were run for six iterations with different smoothing parameters to control the convergence to the final solution.

### 4. Results

Comparing the traveltime residual and RMS misfit provides some insight to the model nonuniqueness because similar data fits are obtained for both final models. However, the traveltime residual of both starting models are different in that the traveltime residual of the layered starting model ( $-0.0043 \pm 0.0117$  s) are worse than the traveltime residual of the gradient starting model ( $0.0017 \pm 0.0075$  s) (Figure 1b). Furthermore, the ray coverage of the latter model is deeper than for the layered starting model (Figure 2). Therefore, we believe that the final model obtained from the gradient starting model is more reasonable for geological interpretation. The obtained source statics that are simultaneously solved for the velocity models are almost independent of the starting model, indicating that this is a robust feature of the dataset. The static terms are derived without any requirement of surface consistency. Despite this, the static shifts show internal consistency and are somewhat correlated with the surface topography as illustrated in Figure 3. For comparison a slice

through a model derived with the preferred starting model but without static shifts is shown in Figure 2b, which shows more model artefacts caused by near surface inhomogeneities.

A cross section through the model along the central receiver line shows a velocity contrast between 1600 m/s and 2000 m/s at the depth of 60-80 m below the surface. Below this boundary, the lateral velocity variations are significant and the lack of the rays coverage in some parts of this layer implies that the model are less reliable. Depth slices through the model at 65, 85 and 105 m below the surface are shown in Figure 4, along with a similarity<sup>1</sup> attribute slice at 150 ms (about 150 m depth) from the processed 3D reflection seismic unit (H. Kazemeini, 2006, pers. comm.).

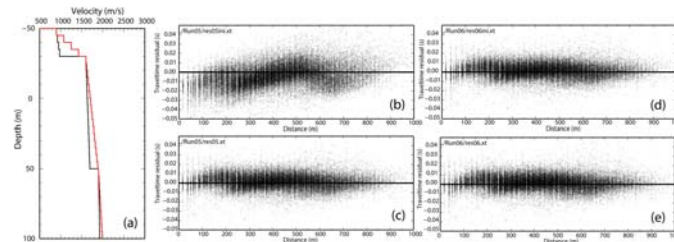


**Figure 1** (a) Layered 1D starting model (black line) and gradient 1D starting model (red line). Traveltime residual versus offset of the layered starting model (b) and the gradient starting model (d). Traveltime residual versus offset of the final model derived from the layered starting model (c) and the gradient starting model (e).

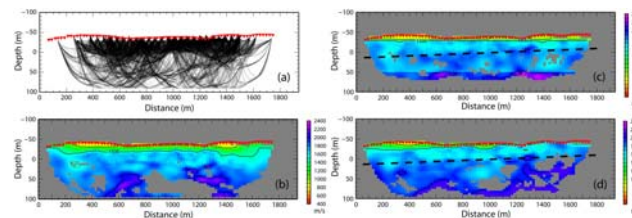


**Figure 2** (a) Ray coverage over a selected profile estimated from the gradient starting model. Note that every 10<sup>th</sup> shot is displayed. (b) Final model inverted using gradient starting model without static shifts. (c) and (d) show the final models inverted using layered and gradient starting models, respectively. Dashed lines mark the interpreted boundary between the Quaternary and Tertiary units.

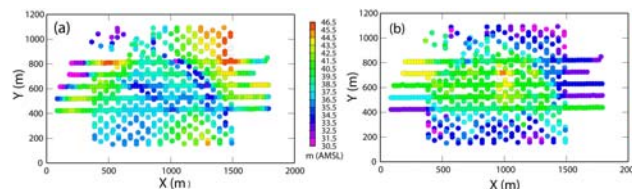


**Figure 3** Topographic map of the study area (a) and shot and receiver static shift associated with near-surface low velocity cover (b). The shot statics are derived simultaneously with the velocity inversion, and the receiver statics (the lines) are derived from the source statics. The two images show some correlation though the static shifts should be more correlated with the thickness of the weathering layer than the topography.

## 5. Discussions and conclusions

The cross section shows the boundary between the Quaternary and Tertiary shallow units, corresponding to the velocity contrast of 1600 and 2000 m/s. The depth slices at depth 85 m and 110 m depth show a trend of low velocities running in approximately an east-west direction in the center of the area (Figure 4). This trend correlates well with the fault trend interpreted from the similarity attribute slice at 150 ms (about 150 m depth). This is an indication that the sedimentary packages higher up than could be imaged in the reflection seismic data are also faulted. The low velocities may be associated with the upward migration of the gas along the fault. However, similar low velocities are observed in other regions of the model, suggesting that more work is needed to establish whether this is the case or not.

In conclusion, our results show that the first-arrival times picked from the 3D reflection seismic data acquired at the Ketzin CO<sub>2</sub> storage site can be used to obtain information on the

<sup>1</sup> Similarity is a form of coherency that expresses how similar two or more adjacent traces are.

inhomogeneous velocity structure of the shallow subsurface which cannot be obtained from the reflection seismic processing. The source statics computed simultaneously with the velocity model are robust and provide information on the thickness of the weathering layer which is new information.

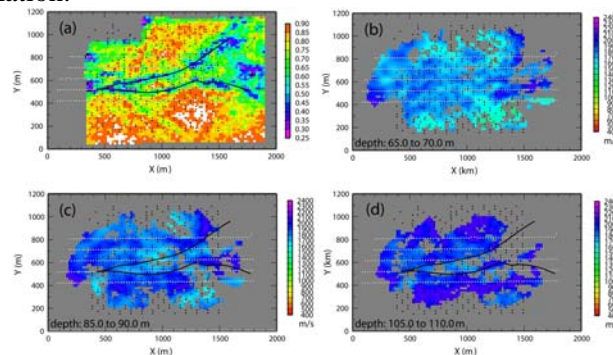


**Figure 4** (a) Similarity attribute slice at 150 ms. The similarity is interpreted as representing faults in the package. (b), (c) and (d) show the tomographic depth slices at selected depths. The fault zones indicated by anomalies in (a) are given by solid lines. Shots and receivers are marked by black dots and white triangles, respectively.

### Acknowledgements

We gratefully acknowledge the CO<sub>2</sub>SINK project for providing us with the supplementary datasets and permission for publication.

### References

- Arts R, Eiken O, Chadwick A, Zweigel P, van der Meer L, and Zinsner B. [2004] Monitoring of CO<sub>2</sub> injected at Sleipner using time lapse seismic data. *Energy* 29, 1383-1392.
- Bergman, B., Tryggvason, A., and Juhlin, C. [2004] High-resolution seismic tomography incorporating static corrections applied to a till covered bedrock environment. *Geophysics* 69, 1082–1090.
- Bergman, B., Tryggvason, A., and Juhlin C. [2006] Seismic tomography studies of cover thickness and near-surface bedrock velocities. *Geophysics* 71, U77–U84.
- Deen, T., and Gohl, K. [2002] 3-D tomographic seismic inversion of a paleochannel system in central New South Wales, Australia. *Geophysics* 67, 1364-1371.
- Förster, A., Norden, B., Zinck-Jørgensen, K., Frykman, P., Kulenkampff, J., Spangenberg, E., Erzinger, J., Zimmer, M., Kopp, J., Borm, G., Juhlin, C., Cosma, C., and Hurter, S. [2006] Baseline characterization of the CO<sub>2</sub>SINK geological storage site at Ketzin, Germany. *Environmental Geosciences* 13, 145-161
- Hole, J.A. [1992] Nonlinear high-resolution three-dimensional reflection seismic travel time tomography. *Journal of Geophysical Research* 97, 6553-6562.
- Juhlin, C., Cosma, C., Förster, A., Giese, R., Juhojuntti, N., Kazemeini, H., Norden, B., and Zinck-Jørgensen, K. [2006] Baseline 3D seismic imaging for the CO<sub>2</sub>SINK project in the Ketzin area, Germany. *Proceedings 8th Greenhouse Gas Technology Conference, Trondheim, Norway*.
- Paige, C.C., and Saunders, M.A. [1982] An algorithm for sparse linear equations and sparse least squares. *ACM Transactions on Mathematical Software* 8, 43–71.
- Podvin, P and Lecomte, I. [1991] Finite different computation of traveltimes in very contrasted velocity models: A massively parallel approach and its associated tools. *Geophysical Journal International* 105, 271-284.
- Tryggvason, A., and Bergman, B. [2006] A travelttime reciprocity discrepancy in the Podvin & Lecomte time3d finite difference algorithm. *Geophysical Journal International* 165, 432–435.
- Yordkayhun, S., Juhlin, C., Giese, R., and Cosma, C. [2006] Shallow velocity-depth model using first arrival travelttime inversion at the CO<sub>2</sub>SINK site, Ketzin, Germany. To be submitted to *Journal of Applied Geophysics*.
- Zelt, C.A., Zaria, A., and Levander, A. [2006] 3D seismic refraction travelttime tomography at a groundwater contamination site. *Geophysics* 71, H67-H78.